Building Supramolecular DNA-Inspired Nanowires on Gold Surface: from 2D to 3D

E. Gatto,*[a] S. Kubitzky,[b] M. Schriever,[b] S. Cesaroni,[a] C. Mazzuca,[a] M. Venanzi,[a] M. De Zotti*[c]

[a] *Department of Chemical Sciences and Technologies, University of Rome "Tor Vergata", 00133 Rome (Italy)*

[b] *Faculty of Engineering and Natural Sciences, Technische Hochschule Wildau, 15745 Wildau (Germany)*

[c] *Institute of Biomolecular Chemistry, Padova Unit, CNR, Department of Chemical Science, University of Padova, 35131 Padova (Italy)*

ABSTRACT. A work of chemical engineering has been realized on gold surfaces. Three building blocks have been designed, in order to chemically link the surface and vertically self assemble in an ordered manner in 3D, through thymine-adenine hydrogen bonds. Starting from these building blocks, we have engineered two different films on gold surface. In film **1**, two components are used: adenine linked to a lipoic acid molecule (Lipo-A) to covalently bind the gold surface, and ZnTPP linked to a thymine molecule (T-ZnTPP). Film **2** has an additional noncovalently linked layer: a helical undecapeptide analogue of the Thricogin GA IV peptide, in which four glycine were replaced by four lysine residues to favor helical conformation and reduce conformational flexibility, and in which the two extremities were functionalized with thymine and adenine, for binding of, respectively, Lipo-A and T-ZnTPP. These films have been characterized by electrochemical and spectroscopic techniques, and have been found to be very stable over time, also in contact with a solution. They were also able to generate current under illumination, with an efficiency higher than the one recorded in similar systems.

The three-dimensional (3D) organization of molecules on surfaces remains an ongoing challenge in the field of materials science.[1] In particular, the molecular order and perfect positioning of

different redox centres may be of fundamental importance in building artificial photosynthetic systems to control the direction of electronic flow.[2-4] Nature uses lipoproteins as a template to organize chlorophyll dyes in an optimal arrangement to avoid strong intermolecular interactions and to confer directionality to the electron transfer (ET) process. All the macromolecules found in nature are constructed by the self-assembly of different building blocks that capitalise on the formation of non-covalent and reversible interactions, including electrostatic, hydrophobic, van der Waals and metal···ligand interactions; hydrogen bonds; and aromatic π-stacking. Collectively, if sufficient in number, these weak interactions can yield highly stable assemblies.[5] A number of studies have investigated ET processes in supramolecular assemblies in solution, similar to those in nature, in which the interacting chromophores are held together by non-covalent interactions.[6] On surface, instead, only electrochemical and spectro-electrochemical properties of 2D self-assembled monolayers (SAMs) covalently linked to a gold surface have been reported [7-16] and very few attempts have been made to build 3D supramolecular structures. Between them, McGimpsey et al.[17] reported on the formation of multilayer thin films on gold via non-covalent interactions between a sulfur-containing 2,6-dicarboxypyridine ligand, a metal ion and other 2,6-dicarboxypyridine ligands, which were used as a means to incorporate one or more layers of pyrene chromophores into the film. This group demonstrated that these films were able to generate a photocurrent with quite high efficiency.[17,18] To our knowledge, no other studies have reported an approach to obtain 3D supramolecular systems on surface, especially systems containing peptides. In this communication, we describe our studies on photocurrent-generating supramolecular components built with an unprecedented approach: we used the thymine-adenine DNA base pair interaction to construct 3D supramolecular films composed of different 2D layers. To this end, we engineered two types of photocurrent-generating films on a gold surface, as shown in Figure 1.

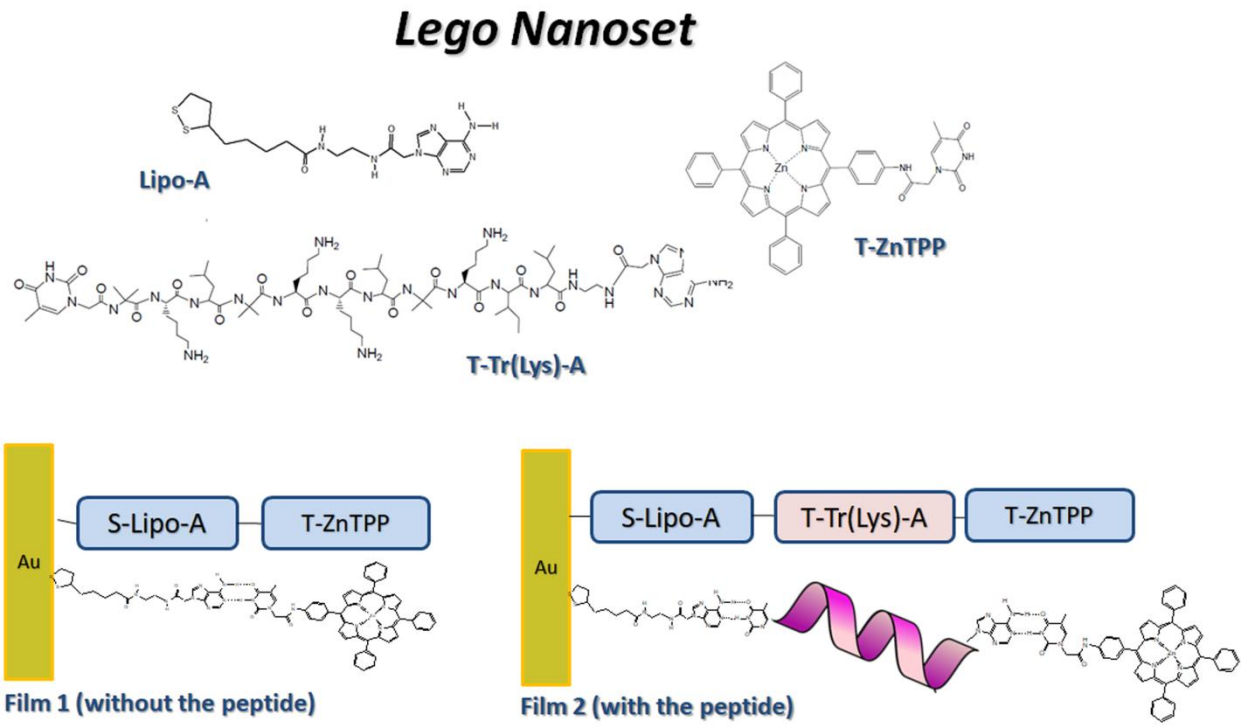

Figure 1. Chemical structures of the building blocks used for the construction of films **1** and **2**.

Films **1** and **2** consist of multi-layered systems in which the light-absorbing group (a zinc-tetraphenylporphyrin chromophore, ZnTPP) is non-covalently linked to a gold surface through thymine-adenine hydrogen bonds. These films are assembled by consecutive deposition of each layer. In film **1**, two components are used: adenine linked to a lipoic acid molecule (Lipo-A) to covalently bind the gold surface and ZnTPP linked to a thymine molecule (T-ZnTPP). Film **2** has an additional non-covalently linked layer: an undecapeptide analogue of the Thricogin GA IV peptide[19] (defined hereafter as T-Tr(lys)-A), in which the four glycine residues were replaced by four lysine residues to favour helical conformation[20] (Supporting Information, Figure S1) and reduce conformational flexibility, and the two extremities were functionalized with thymine and adenine for binding of Lipo-A and T-ZnTPP, respectively. Experimental details on the synthesis of molecular components and the film depositions are provided in the Supporting Information. Other groups who investigated similar systems in solution were able to form long filaments through thymine-adenine interaction by properly tuning the experimental conditions.[21]

Conductivity, infrared reflection absorption spectroscopy (IR-RAS), ultraviolet-visible (UV-vis) and fluorescence spectroscopy measurements were carried out for films **1** and **2** after the formation of each layer. Cyclic voltammetry (CV) experiments performed in a 0.1 M acetate buffer solution at pH 4.4 evaluated the Lipo-A density on the surface.[22] By measuring the amount of charge required for complete oxidation of adenine, we obtained a molecular density of $(7.3\pm0.8)\cdot10^{-10}$ mol/cm^2 by taking into account the electrode effective surface area, which is 1.1 times larger than the geometric one (Figures S2 and S3, Supporting Information).[5] From this value, the mean area occupied by a single molecule on the surface is (23±1) Å^2. This value can be used to determine the adenine molecular orientation on the gold surface, taking into account the size of the molecules (treated as a parallelepiped): 50 Å^2 in a horizontal arrangement and 22 Å^2 in a vertical arrangement. From such evaluations, it is concluded that the Lipo-A molecules are densely packed with a perpendicular orientation to the gold surface. The Fourier transform infrared reflection absorption spectroscopy (FTIR-RAS) measurements assessed the presence of the peptide layer and determined its conformation and molecular orientation on the surface. The obtained FTIR-RAS spectrum is shown in Figure 2.

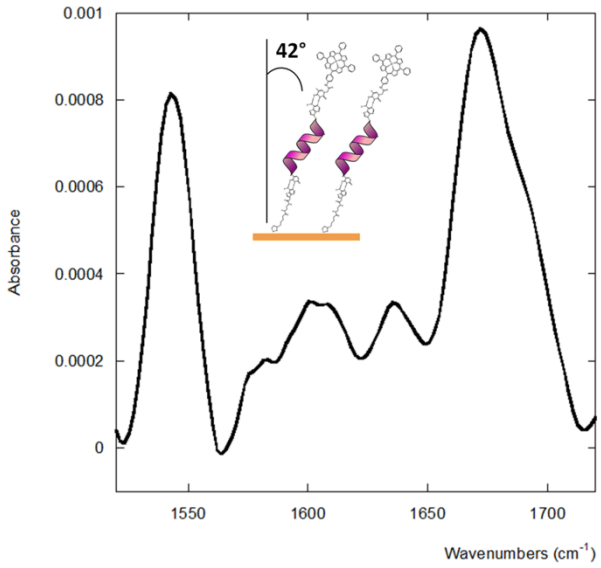

Figure 2. IR-RAS spectrum of film **2**.

Amide I and amide II bands appeared at 1543 cm^{-1} and 1673 cm^{-1}, respectively, confirming the presence of a peptide layer on the surface; in particular, these results indicate an α-helix positioned vertically on the substrate surface.[13b] Calculations based on the amide I/amide II absorbance ratios led to the following tilt angle of the helix axis normal to the surface: 42°. This value is generally obtained for very good self-assembled peptide monolayers, indicating that the T-Tr(lys)-A peptide forms a homogeneous film on the Lipo-A layer.[23-25] Interestingly, in film **1,** these signals are much less intense due to the lower content of amide bonds, confirming the presence of the intermediate layer of film **2**. The difference between the spectrum obtained by the IR-RAS measurements of film **2** and that of film **1** is reported as Supporting Information, Figure S4.

The presence of the third layer was evaluated by two different methods: first, the film was deposited on a gold (5 nm)-coated glass slide to perform absorption and fluorescence spectroscopy measurements. The absorption spectra not only confirmed the presence of the T-ZnTPP molecule but also determined the amount of porphyrin molecules from the measured absorbance value.[26] This value was $(7.0\pm0.5)\cdot10^{-11}$ mol/cm^2 for film **1** and $(3.5\pm0.8)\cdot10^{-11}$ mol/cm^2 for film **2** (with the peptide). The fluorescence emission spectra confirmed that the absorption bands were those of the porphyrin ring (Supporting Information, Figure S5). The different surface densities of T-ZnTPP in films **1** and **2** were also measured by detaching the film from the gold surface by CV (Supporting Information) and analysing the visible absorption spectrum of the electrolytic solution after film removal. From the absorption spectrum, the known solution volume and electrode immersion area and by taking into account the electrode surface roughness, the Γ values were determined. The results are reported in Figure S6 and in Table 1.

Table 1. Results obtained using UV-vis absorption spectroscopy in transmission mode (directly on surface and after film removal in solution) and photoelectrochemical measurements.

System	Absorbance	Γ (mol/cm^2) from absorbance on surface	Γ (mol/cm^2) from absorbance in solution	Photocurrent Intensity (nA/cm^2)	Quantum yield (430 nm) using absorbance value
Film **1**	0.035	$7.0\pm0.5\times10^{-11}$	$8.5\pm1.5\times10^{-11}$	109	0.3% (0 V) 0.4% (-0.3 V)
Film **2**	0.018	$3.5\pm0.8\times10^{-11}$	$4.1\pm1.3\times10^{-11}$	175	1.0% (0 V) 2.3% (-0.3 V)

Herein, to demonstrate the capability of our SAM to give rise to oxygen photoreduction, we performed photocurrent generation measurements in the ZnTPP absorption range. Photocurrent responses of film **1** and film **2** are shown in Figure 3.

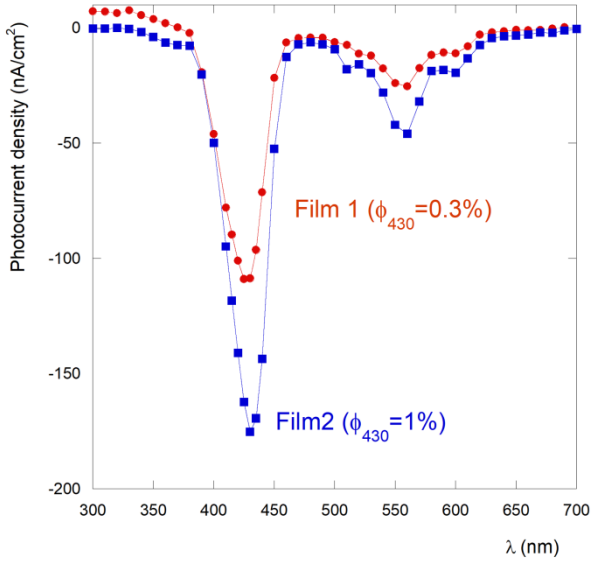

Figure 3. Photocurrent action spectra of film **1**/Au/TEOA/Pt and film **2**/Au/TEOA/Pt cells.

We found that upon illumination in the visible region and in the presence of a stable and non-corrosive electron donor (triethanolamine, TEOA), high cathodic currents were generated.[27] The photocurrent action spectrum is very similar to the surface absorption spectrum of ZnTPP, confirming that ZnTPP is the photoexcited species responsible for the signal. The electron acceptor in the present system is supposed to be O_2 in solution (Figure 4a). To confirm this hypothesis, we performed the same photocurrent generation experiments by exciting the samples at 420 nm after fluxing for 20 minutes with argon into the solution. The oxygen removal produced a large decrease in the photocurrent signal, confirming our assumption (Figure 4b).[28] Interestingly, a significant enhancement in the magnitude of the photocurrent upon inserting the peptide between Lipo-A and the deposited T-ZnTPP SAM is clearly observed, with film **2** having a higher

photocurrent value (175 nA/cm^2 at 430 nm) than film **1** (109 nA/cm^2 at 430 nm), despite the lower ZnTPP content shown by surface absorption spectroscopy both on surface (Table 1) and after film removal in solution (Table 1). These values are higher than those reported for ZnTPP systems on both indium tin oxyde (ITO)[29] and gold[30] surfaces and represent a quantum efficiency at 430 nm[9] of 1.0% for film **2** and 0.3% for film **1**.[31] When a negative potential was applied, the efficiency increased, reaching 2.3% for film **2** and 0.4% for film **1** at an applied potential of -0.3 V**.** These values are higher than those obtained with other porphyrin-peptide systems covalently linked to a gold surface.[15a,b]

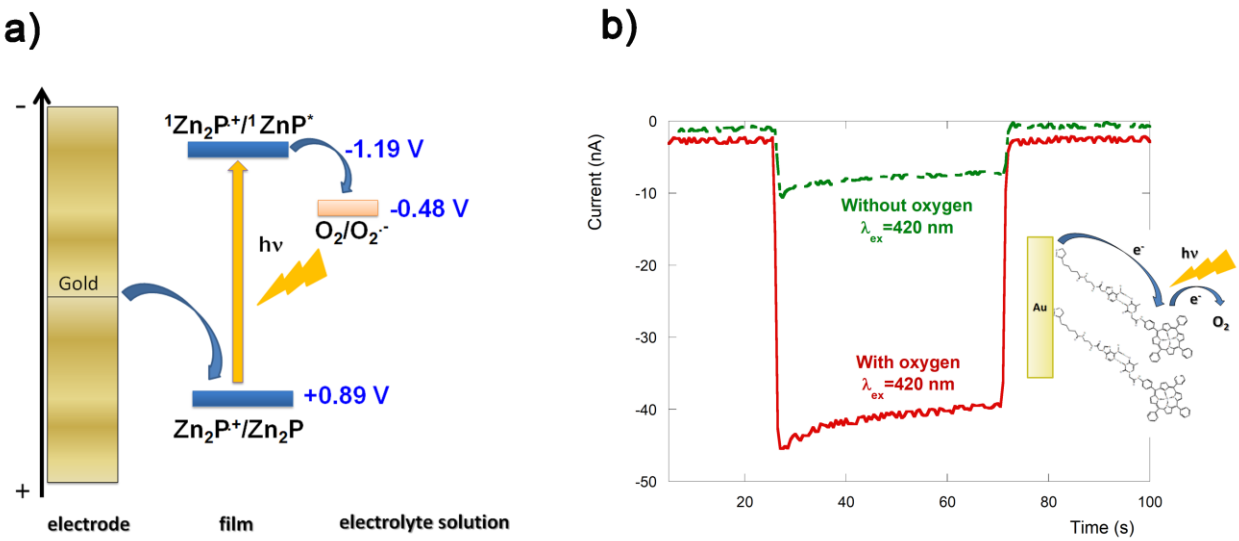

Figure 4. a) Photocurrent generation diagram indicating the path of the electron flow; b) photocurrent signal obtained by exciting film **1** at 420 nm before and after oxygen removal (inset: scheme of the electron flow).

The reason for the higher photocurrent value obtained with the peptide-containing film might be multi-fold. First, it is well known that the porphyrin-excited singlet state is quenched by the gold electrode via energy transfer. This process depends on distance and should be more efficient with film **1**, in which the ZnTPP is closer to the gold surface, giving rise to a lower photocurrent value. In contrast, the ET rate from the gold electrode to the resulting porphyrin cation radical decreases with an increase in chain length, favouring a higher photocurrent value in film **1**. Third, the presence of porphyrin aggregation enhances the rate of the nonradiative pathway in the excited state. The presence of J-aggregates in films **1** and **2** is suggested by the surface absorption spectrum (10 nm shift) and by the maximum photocurrent absorption (which is approximately 430 nm in both films). However, the mean molecular area occupied by the T-ZnTPP layer in the two films is different, being 240 Å^2 for film **1** and 476 Å^2 for film **2**. This difference suggests that the porphyrin molecular orientation on the gold surface in the two films is different (the size of the molecule is 480 Å^2 in a planar arrangement and 200 Å^2 in a vertical arrangement).[30] It has already been demonstrated that porphyrin aggregation and molecular orientation influence photocurrent efficiency.[30,32]

Repeated photoexcitation of films **1** and **2** results in a 25-55% loss in photocurrent intensity after approximately 8 hours of measurements of alternating light/dark cycles and at different applied voltages. Interestingly, the day after the measurements, the photocurrent intensities of both films were recovered, suggesting that the films were stable (Figure S8). The films were found to be very stable, giving rise to the same photocurrent intensity (using a fresh electrolyte solution) for more than two months (stored at ambient temperature). Therefore, we interpreted the current decrease observed after several hours of measurements as oxygen consumption. Notably, however, all these results clearly indicate that the bio-inspired non-covalent strategy developed in the present work is a potentially effective and simple means by which to engineer complex modular supramolecular SAMs to control film length for device fabrication purposes, including the conversion of incident light to electronic current and oxygen photoreduction for photodynamic therapy.

ASSOCIATED CONTENT

Circular dichroism spectrum of T-Tr(lys)-A in methanol, cyclic voltammetry of lipo-adenine on the surface, IR-RAS spectral difference of the two films, UV-visible absorption and fluorescence spectra of the two films on the surface, cyclic voltammetry of films 1 and 2 on the gold surface, synthesis of all the building blocks and their HPLC and NMR characterization, TEM images of the fibres formed by T-Tr(lys)-A in acetonitrile, and experimental details. This material is available free of charge via the internet at http://pubs.acs.org.

AUTHOR INFORMATION

Corresponding authors: Emanuela Gatto: emanuela.gatto@uniroma2.it; Marta De Zotti: marta.dezotti@unipd.it

NOTES

The authors declare that they have no competing financial interests.

ACKNOWLEDGEMENT

This work was supported by MIUR (Rome, Italy) (Futuro in Ricerca 2013, grant no. RBFR13RQXM).

REFERENCES

1. J. Martin, M. Martin-Gonzalez, J. F. Fernandez, O. Caballero-Calero, *Nat. Commun.* **2014**, 5130.
2. (a) M. Morisue, S. Yamatsu, N. Haruta, Y. Kobuke, *Chem. Eur. J.* **2005**, *11*, 5563-5574. (b) D. M. Guldi, *Chem. Soc. Rev.* **2002**, *31*, 22-36. (c) W. Kim, E. Edri, H. Frei, *Acc. Chem. Res.* **2016**, *49*, 1634–1645.
3. M. E. El-Khouly, E. El-Mohsnawy, S. Fukuzumi, *J. Photochem. Photobiol. C: Photochem. Rev.* **2017**, *31*, 36-83.

4. (a) V. Balzani, A. Credi, M. Venturi, *ChemSusChem.* **2008**, *1*, 26–58; (b) J. Barber, *Chem Soc Rev.* **2009**, *38*, 185–196.
5. (a) J. M. Lehn, *PNAS* **2002**, *99*, 4763-4768; (b) G. M. Whitesides, J. P. Mathias, C. T. Seto, *Science* **1991**, *254*, 1312-1319; (c) J. M. Lehn, *Science* **2002**, *295*, 2400-2403; (d) G. M. Whitesides, B. Grzybowski, *Science* **2002**, *295*, 2418-2421.
6. (a) M. R. Wasielewski, *Acc. Chem. Res.* **2009**, *42*, 1910–1921; (b) M. D. Ward, *Chem. Soc. Rev*. **1997**, *26*, 365-375.
7. (a) R. G. Nuzzo, D. L. Allara, *J. Am. Chem. Soc.* **1983**, *105*, 4481-4483; (b) L. H. Dubois, R. G. Nuzzo, *Annu. Rev. Phys. Chem.* **1992**, *43*, 437-463; (c) M. D. Porter, T. B. Bright, D. L. Allara, C. E. D. Chidsey, *J. Am. Chem. Soc.* **1987,** *109*, 3559-3568; (d) E. P. Enriquez, C. H. Gray, V. F. Guarisco, R. V. Linton, D. K. Mar, E. T. Samulski, *J. Vac. Sci. Technol.* **1992**, *10*, 2775-2782.
8. Y. T. Long, E. A. Irhayem, H. B. Kraatz, *Chem. Eur. J.* **2005**, *11*, 5186-5194.
9. E. Gatto, A. Porchetta, M. Scarselli, M. De Crescenzi, F. Formaggio, C. Toniolo, M. Venanzi, *Langmuir* **2012**, 28, 2817-2826.
10. a) M. Venanzi, G. Pace, A. Palleschi, L. Stella, P. Castrucci, M. Scarselli, M. De Crescenzi, F. Formaggio, C. Toniolo, G. Marletta, *Surface Sci.* **2006**, *600*, 409-416; b) E. Gatto, L. Stella, C. Baldini, M. Venanzi, C. Toniolo, F. Formaggio, *Superlatt. Microstruct.* **2009**, *46*, 34-39.
11. (a) N. Amdursky, *ChemPlusChem* **2015**, *80*, 1075-1095; (b) A. Shah, B. Adhikari, S. Martic, A. Munir, S. Shahzad, K. Ahmad, H. B. Kraatz, *Chem. Soc. Rev.* **2015**, *44*, 1015-1027; (c) H. S. Mandal, H. B. Kraatz, *J. Phys. Chem. Lett.* **2012**, *3*, 709–713.
12. E. Gatto, M. Caruso, M. Venanzi, *The Electrochemistry of Peptide Self-Assembled Monolayers.* In: Aliofkhazraei M., Makhlouf A. (eds) Handbook of Nanoelectrochemistry. Springer, Cham., **2016**.
13. (a) S. Sek, A. Tolak, A. Misicka, B. Palys, R. Bilewicz, *J. Phys. Chem. B* **2005**, *109*, 18433–18438; (b) J. Watanabe, T. Morita, S. Kimura, *J. Phys. Chem. B* **2005**, *109*, 14416–14425; (c) S. Sek, A. Sepiol, A. Tolak, A. Misicka, R. Bilewicz, *J. Phys. Chem. B* **2004**, *108*, 8102–8105; (d) Y. Arikuma, K. Takeda, T. Morita, M. Ohmae, S. Kimura, *J Phys Chem B* **2009**, 113, 6256–6266; (e) H. S. Mandal, H. B. Kraatz, *Chem. Phys.* **2006**, *326*, 246–251; (f) Y. Arikuma, H. Nakayama, T. Morita, *Angew. Chem. Int. Ed.* **2010**, *49*, 1800–1804; (g) Y. Arikuma, H. Nakayama, T. Morita, S. Kimura, *Langmuir* **2011**, *27*, 1530–1535.
14. (a) S. Yasutomi, T. Morita, Y. Imanishi, S. Kimura, *Science* **2004**, *304*, 1944-1947; (b) T. Morita, S. Kimura, S. Kobayashi, Y. Imanishi, *J. Am. Chem. Soc.* **2000**, *122*, 2850–2859; (c) K. Yanagisawa, T. Morita, S. Kimura, *J. Am. Chem. Soc.* **2004**, *126*, 12780–12781; (d) S. Yasutomi, T. Morita, S. Kimura, *J. Am. Chem. Soc.* **2005**, *127*, 14564–14565.
15. (a) H. Uji, Y. Yatsunami, S. Kimura, *Phys. Chem. C* **2015,** *119*, 8054-8061; (b) H. Uji, K. Tanaka, S. Kimura, *J. Phys. Chem. C* **2016**, *120*, 7, 3684-3689; (c) M. Venanzi, E. Gatto, M. Caruso, A. Porchetta, F. Formaggio, C. Toniolo, *J. Phys. Chem. A* **2014**, *118*, 6674-6684.
16. (a) H. Imahori, Y. Nishimura, H. Norieda, H. Karita, I. Yamazaki, Y. Sakata, S. Fukuzumi, *Chem. Commun.* **2000**, 661-662; (b) H. Imahori, H. Norieda, Y. Nishimura, I. Yamazaki, K. Higuchi, N. Kato, T. Motohiro, H. Yamada, K. Tamaki, M. Arimura, Y. J. Sakata, *J. Phys. Chem. B* **2000**, *104*, 1253-1260; (c) H. Imahori, H. Norieda, H. Yamada, Y. Nishimura, Y. J. Sakata, S. Fukuzumi, *J. Am. Chem. Soc.* **2001**, *123*, 100–110.
17. E. Soto, J. C. MacDonald, C. G. F. Cooper, W. G. McGimpsey, *J. Am. Chem. Soc.* **2003**, *125*, 2838-2839.
18. P. F. Driscoll, Jr., E. F. Douglass, M. Phewluangdee, E. R. Soto, C. G. F. Cooper, J. C. MacDonald,. C. R. Lambert, W. G. McGimpsey, *Langmuir* **2008**, *24*, 5140–5145.
19. C. Peggion, F. Formaggio, M. Crisma, R. F. Epand, R. M. Epand, C. Toniolo, *J. Pept. Sci.* **2003**, *9*, 679-689.

20. M. De Zotti, B. Biondi, C. Peggion, F. Formaggio, Y. Park, K. S. Hahm, C. Toniolo, *Org. Biomol. Chem.* **2012**, *10*, 1285-1299.
21. (a) G. Marafon, D. Mosconi, D. Mazzier, B. Biondi, M. De Zotti, A. Moretto, *RSC Adv.* **2016**, *6*, 73650-73659; (b) G. Marafon, I. Menegazzo, M. De Zotti, M. Crisma, C. Toniolo, A. Moretto, *Soft Matter* **2017**, *13*, 4231-4240.
22. A. M. Oliveira-Brett, V. Diculescu, J. A. P. Piedade, *Bioelectrochemistry* **2002***, 55*, 61–62.
23. M. Kai, K. Takeda, T. Morita, S. Kimura, *J. Pepti. Sci.* **2008**, 14, 192-202.
24. S. Okamoto, T. Morita, S. Kimura, *Langmuir* **2009**, 25, 3297-3304.
25. K. Takeda, T. Morita, S. Kimura, *J. Phys. Chem. B* **2008**, 112, 12840-12850.
26. F. Sabuzi,; V. Armuzza, V. Conte, B. Floris, M. Venanzi, P. Galloni, E. Gatto, *J. Mater. Chem. C*, **2016**,*4*, 622-629.
27. In general TEOA solutions give rise to anodic photocurrent. However, it has been demonstrated in the literature that different porphyrin SAMs favor ET to O_2 in solution, due to the similar electrochemical potential of TPP and TEOA.
28. A. Vecchi, E. Gatto, B. Floris, V. Conte, M. Venanzi, V. N. Nemykin, P. Galloni, *Chem. Commun*. **2012**, *48*, 5145-5147.
29. (a) H. Yamada,; H. Imahori,; Y. Nishimura, I. Yamazaki,; S. Fukuzumi, *Advanced Mater.* **2002**, *14*, 892-895; (b) H. Imahori, M. Kimura, K. Hosomizu, T. Sato, T. K. Ahn, S. K. Kim, D. Kim, Y. Nishimura, I. Yamazaki, Y. Araki, O. Ito, S. Fukuzumi, *Chem. Eur. J.* **2004**, *10*, 5111 – 5122.
30. (a) H. Imahori, H. Norieda, Y. Nishimura, I. Yamazaki, K. Higuci, N. Kato, T. Motohiro, H. Yamada, K. Tamaki, M. Arimura, Y. Sakata, *J. Phys. Chem. B* **2000**, *104*, 1253–1260; (b) H. Imahori, T. Hasobe, H. Yamada, Y. Nishimura, I. Yamazaki, S. Fukuzumi, *Langmuir* **2001**, *17*, 4925-4931.
31. The quantum efficiency has been calculated using the absorption values obtained by UV-Vis measurements on surface. Using the surface coverage obtained by CV measurements, higher quantum efficiencies are obtained, with the film **2** value still higher than that of film **1**.
32. B. J. Walker, A. Dorn, V. Bulović, M. G. Bawendi, *Nano Lett.* **2011**, *11*, 2655–2659.